International Journal of Sensors and Sensor Networks
2019; 7(1): 1-8
http://www.sciencepublishinggroup.com/j/ijssn
doi: 10.11648/j.ijssn.20190701.11
ISSN: 2329-1796 (Print); ISSN: 2329-1788 (Online)

SciencePG
Science Publishing Group

Research/Technical Note

A Portable Sensor for Skin Bioimpedance Measurements

Joshua Robert Harvey, Yitzhak Mendelson

Department of Biomedical Engineering, Worcester Polytechnic Institute, Worcester, USA

Email address:
jrharvey@wpi.edu (J. R. Harvey), ym@wpi.edu (Y. Mendelson)

To cite this article:
Joshua Robert Harvey, Yitzhak Mendelson. A Portable Sensor for Skin Bioimpedance Measurements. *International Journal of Sensors and Sensor Networks*. Vol. 7, No. 1, 2019, pp. 1-8. doi: 10.11648/j.ijssn.20190701.11

Received: July 1, 2019; **Accepted**: July 25, 2019; **Published**: August 10, 2019

Abstract: The costs of pressure injury treatments continue to rise with a steadily aging population and consistent pressure injury incidence rates. Evidence suggests that the bioimpedance of living tissues changes in response to continuous pressure loading and may be useful as an indicator for the onset of pressure injuries. Therefore, the development of a low-cost, accurate, and portable sensor capable of measuring the bioimpedance of human skin has practical significance in the development of pressure injury prevention devices. This paper reports the design and characterization of a system for measuring skin impedance based on the AD5933 impedance analyzer. The sensor was tested for accuracy via measurements of a simplified electrical equivalent skin model. Long duration measurement stability was assessed over 24 hours and skin measurement repeatability was performed on the volar forearm. The power consumption was measured both during idle and when transmitting data for each major component. The sensor demonstrated accuracies similar to those reported for other AFE's used in conjunction with the AD5933. Additionally, the sensor shows good stability over long measurement durations as well as good repeatability when measuring the skin bioimpedance on the volar forearm. Power consumption was as expected and future suggestions for lowering the overall circuit power consumption and size are presented.

Keywords: Bioimpedance, Portable, Skin, Pressure, Ulcer

1. Introduction

In an aging population, the number of individuals at risk of developing pressure-induced injuries is steadily increasing. Pressure injuries (also known as pressure ulcers, decubitus ulcers, bed sores) are localized damage to the skin and underlying soft tissues caused by excessive pressure, shear, or a combination of the two for a prolonged duration. These injuries typically form over a boney prominence such as the sacrum, heels, and occipital bone. Clinically, the gold standard of care is to rotate individuals every two hours if they are considered at risk of developing these wounds. However, incidence rates of pressure injuries are still as high as 12% in the U.S. [1]. Pressure injuries are painful, increase likelihood of secondary infection, and cost the U.S. health care system 11 billion dollars annually [2]. Visual inspection by trained nursing staff is the gold standard for pressure injury detection, which can lag the pressure loading event by several days to weeks. This delay, as well as the subjective nature of visual inspections, has led researchers to investigate various alternative non-invasive monitoring techniques such as ultrasound, thermography, photography, and sub-epidermal moisture (SEM) [3-6]. While these techniques have shown promise, and in the case of SEM, earlier detection [7], versus visual inspection alone, the main drawback is that these techniques require observation of the wound healing response in order to detect impending or existing ulceration. No system currently exists that can continuously monitor an individual and alert them or a clinician before tissue damage may result in a pressure injury.

Bioimpedance is the technique of measuring the electrical properties of living tissues. It has been used in pressure injury research as a method of assessing ulcer formation noninvasively [8, 9]. By measuring the electrical properties of tissues, insight into the relative proportions of intracellular and extracellular fluids as well as the relative capacitive nature of the tissue can be used to indicate inflammation and tissue damage. While bioimpedance is an attractive method for continuously assessing tissue properties, commercial impedance analyzers are expensive and too large for remote

monitoring or large scale clinical deployment. Many researchers have turned to cheaper alternatives such as designing analog front ends (AFE) for the AD5933, an impedance analyzer on an integrated circuit (IC) from Analog Devices [10-15]. Many of these circuits change the output of the AD5933 IC into a constant current source and measure tissue impedance using a four-electrode configuration with two current sourcing electrodes and two voltage sensing electrodes. While the accuracies and stability of these devices performs well within their desired frequency range, many of these circuits do not cover most of the expected impedance range of skin and some circuits may be difficult to miniaturize. Additionally, many of these devices utilize instrumentation amplifiers that require at least 5V for operation.

The purpose of this work is to develop and characterize a low-cost, portable, and wireless sensor for measuring noninvasively human skin bioimpedance. Such a device would enable safe and reliable measurements in a small form factor for remote monitoring of skin bioimpedance. The circuit proposed in this paper can operate on a single 3.7 V Lithium source, making it a viable option for remote monitoring of pressure-induced injuries. The long term goal is to be able to monitor changes in skin bioimpedance, in conjunction with other indicators, and alert individuals or care takers of the risk for developing pressure-induced injuries.

2. Materials and Methods

2.1. Bioimpedance

Bioimpedance is the ability of biological tissue to impede an electric current. It is broadly used in body composition measurements and healthcare assessment systems [16-18]. These noninvasive systems source a small amount of alternating current into human tissues and measure the resulting voltage. From the sourced current and measured voltage, one can determine the electrical properties of the underlying tissues. From an electrical standpoint, impedance (Z) is the effective resistance to an alternating current. It is dependent on the frequency of the alternating current, and it is commonly defined by its magnitude ($|Z|$) and phase angle (θ) [18]. The relationships between Z, $|Z|$, and θ are defined by Equations (1-3). Bioimpedance (Z) is a complex quantity composed of the real resistance component (R), which is primarily attributed to total body water and the imaginary reactance component (X_c), which is attributed to the lumped capacitance of cell membranes [19]. Phase angle (θ), similar to reactance, represents the ability of a tissue to store charge. Studies have shown that damaged tissues exhibit lower overall impedance, reactance, and phase angle (closer to zero) [8, 20, 21]. This has been described as a disturbance of biological structures, particularly the destruction of healthy cell membranes which leads to increased ion flow and reduced capacitance.

$$Z = R + jX_C \tag{1}$$

$$|Z| = \sqrt{R^2 + X_C^2} \tag{2}$$

$$\theta = tan^{-1}\left(\frac{X_C}{R}\right) \tag{3}$$

The two primary configurations for bioimpedance measurements are based on two and four electrode systems. In a two electrode system, the two voltage sourcing electrodes are applied to the skin and the resultant current is measured. Four electrode configurations are typically a collinear arrangement of two outer current sourcing and two inner voltage sensing electrodes. While the four electrode arrangement will perform better when measuring a homogeneous medium, this configuration may lose accuracy in heterogeneous mediums. The “current path problem” exists when the current between sourcing electrodes takes a path of least resistance that is not near the collinear electrode arrangement which results in erroneously low voltages at the sensing electrodes. In a two electrode system, the current is required to pass between the two electrodes. Additionally, the two electrode setup can be used in an electrode grid configuration with lower complexity to switch between electrode pairs. One major drawback of using a two electrode arrangement, particularly for frequencies below 20 kHz [22], is the inclusion of electrode interface impedance in the measurement. However, the impact of this phenomenon is reduced by measuring at frequencies above 20 kHz as well as observing the difference between bioimpedance measures over time. In this way, it is not the absolute impedance that is of critical importance but rather the change in impedance as tissues are subject to external loading. It is also possible to reduce the electrode impedance effect by utilizing more than one set of electrodes with different separation distances and subtracting the results from each pair for single time point measurements [23]. For these reasons, a two electrode configuration was chosen for the portable skin bioimpedance sensor.

2.2. Materials and Experiments

The design of the portable bioimpedance sensor is based on several important criteria. The device must be power efficient, low voltage, and capable of measuring typical skin impedance values. In order to meet these criteria, the device was designed to be able to measure impedance values between 200 Ω and 100 kΩ which are typical skin impedances for frequencies between 1 kHz and 100 kHz [24, 25]. The sensor was designed to operate at 3.3V such that the device could be powered via a single 3.7 V Lithium ion cell. Labeled pictures of the physical device are shown in Figure 1. The sensor is based around the AD5933 impedance analyzer IC from Analog Devices. The AD5933, powered by a 3.3 V source, can provide sinusoidal voltage waveforms with peak-to-peak voltage (Vpp) values of 200 mV, 400 mV, 1 V, and 2 V with varying DC offsets. The output of the AD5933 first passes through a high pass filter in order to remove the varying DC offset and is raised to a fixed DC offset of half the input voltage to improve the dynamic range. Next, the signal is amplified by an inverting amplifier whose feedback resistor is controlled by an ADG704 4-channel multiplexer, providing gains of ¼, ½, 1, and 1.5.

This allows the system to produce sinusoidal waveforms with a Vpp of 25 mV, 50 mV, and 3 V, in addition to the native settings. This signal is then applied across an unknown impedance, such as human skin, which results in a current that passes through the trans-impedance amplifier (TIA). The TIA assures that the DC bias voltage across the unknown impedance is near zero, amplifies the small current, translates the current into a voltage, and limits the maximum current that can pass via choice of its feedback resistor (R_4). The resulting voltage waveform is then passed through a resistor (R_5) and into the AD5933's TIA with an effective gain of 1. While it may seem redundant to use two back-to-back TIA circuits, the DC offset of the AD5933's internal TIA is internally fixed and in our testing did not provide the DC offset required for the highest dynamic range. A simplified schematic representing the operation of the circuit is shown in Figure 2.

The Arduino Nano was chosen as the main processing unit to control the AD5933 and inverting amplifier feedback multiplexer as well as communicate with a PC. Wireless communication was performed using an HC-06 Bluetooth module. Although there are more power efficient processors and communication protocols, this prototype provides a simple low-cost platform for demonstrating proof-of-concept.

The resulting sensor is capable of measuring impedances between 180 Ω and 165 kΩ by manipulating the Vpp of the input voltage. The device attempts to measure an unknown impedance at the largest Vpp first since a larger Vpp led to better signal-to-noise ratios. If the first measurement attempt results in a reading that is too large, this indicates that the ADC of the AD5933 is saturating and the Vpp is lowered. Conversely, if a reading is too small, the input voltage Vpp is increased. This configuration allows automatic range changing without prior knowledge of the unknown impedance. All measurement ranges overlap so there are no gaps in the measurable impedance range.

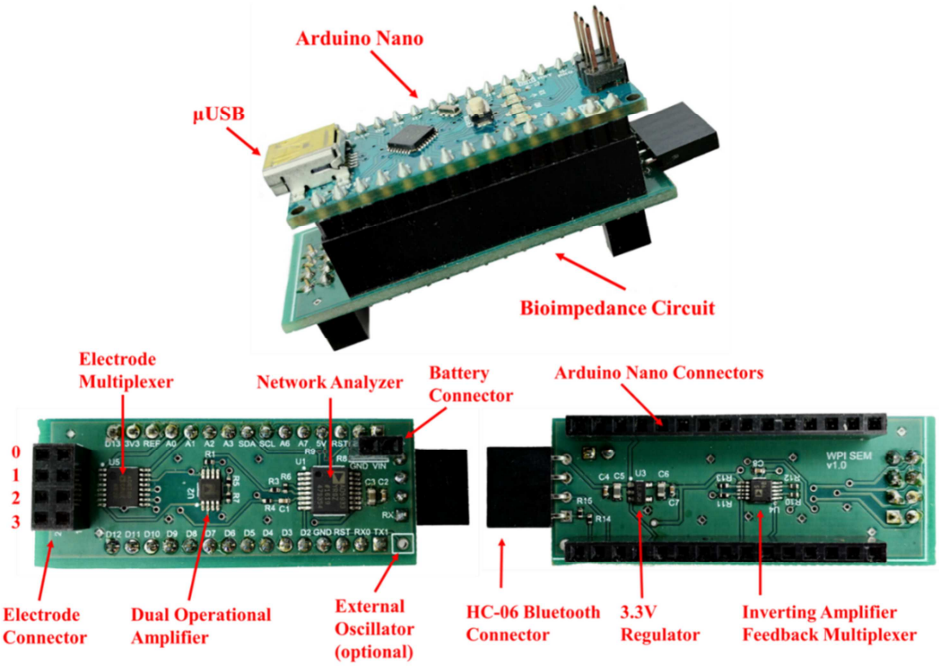

Figure 1. *Labeled pictures of sensor and Arduino Nano. HC-06 is not shown.*

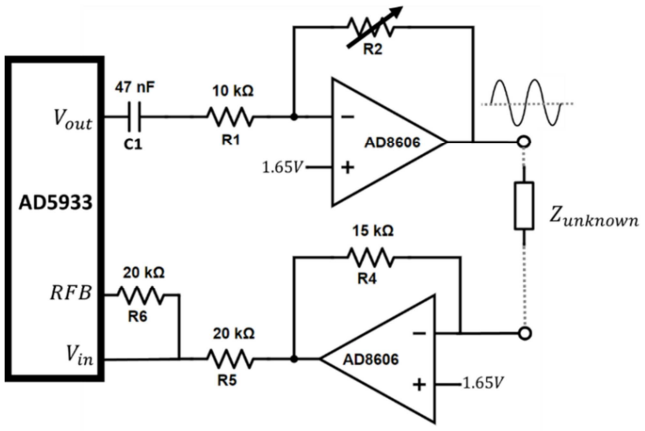

Figure 2. *Simplified sensor schematic for measuring the bioimpedance of human skin.*

3. Results

3.1. Bioimpedance Circuit Calibration

The sensor was calibrated by recording the real and imaginary components of the Discrete Fourier Transform (DFT), reported by the AD5933, of measurements from an array of known resistors. In order to translate the real and imaginary components acquired from the DFT into actual impedance values, gain factors were calculated. Gain factors were calculated by relating known impedance values to the magnitude of the complex value reported via the DFT for each frequency, as defined in Equation 4 [26]. Phase angle offsets were also calculated to account for phase shifts caused by the measurement circuitry. Phase angle offsets were calculated as defined in Equation 5. Resistors are used for calibration since

their electrical properties are independent of the measurement frequency.

$$Gain\ Factor_j = \frac{1}{Impedance \cdot \sqrt{R_j^2 + I_j^2}} \quad (4)$$

$$Phase\ Offset_j = \tan^{-1}\left(\frac{I_j}{R_j}\right) \quad (5)$$

for j = 5, 6,…, 100 kHz, where R and I represent the real and imaginary component of the DFT, respectively.

After gain factors and phase offsets were calculated using known calibration resistor values, linear fits were constructed. For each Vpp voltage setting, three resistors were measured for frequencies ranging between 5 kHz to 100 kHz in 1 kHz increments. The resistor values were chosen at the minimum, median, and maximum impedances that the Vpp voltage setting is capable of measuring. Linear fits were computed between subsequent calibration points and were used to determine the impedance magnitude and phase angle of the measured unknown impedances.

3.2. Accuracy

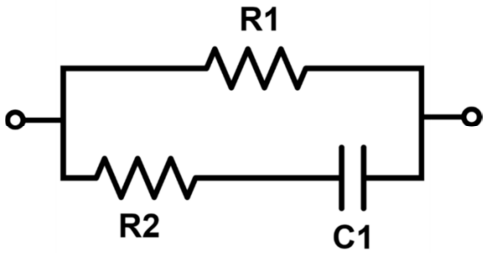

Figure 3. *Accuracy test circuit.*

In order to determine the sensor's accuracy, sets of resistors and capacitors were chosen such that for each Vpp output voltage setting the entire effective range would be swept when the frequency was changed from 5 kHz to 100 kHz. Additionally, this circuit configuration represents a simplified electrical equivalent model for the dispersion and absorption in polar mediums [27]. The test circuit configuration is shown in Figure 3.

Accuracy is reported as absolute impedance error and absolute phase error, defined in Equations (6-7).

$$|Impedance\ Error| = \frac{|Z_{theo}| - |Z_{meas}|}{|Z_{theo}|} \cdot 100 \quad (6)$$

$$|Phase\ Angle\ Error| = |\theta_{theo}| - |\theta_{meas}| \quad (7)$$

Initial measurements for Vpp voltage settings of 25 mV, 50 mV, and 200 mV required capacitances of 10 nF, 10 nF, and 1.5 nF, respectively, in order to sweep the entire impedance range. However, these capacitances are much larger than reported locale skin capacitances ranging between 10's to 100's pF and cause op-amp instability due to self-oscillation which can lead to large errors. Here, we are showing measurements at those voltage settings with the capacitor set to a value of 100 pF which represents a small impedance change over the entire frequency sweep and a lower capacitive load which is more appropriate for the intended bioimpedance application. The largest capacitive load used in these tests was 1 nF for the 400 mV setting. Measured values of the components used for each Vpp setting, as well as the measured maximum and minimum impedance and phase angles are shown in Table 1. This illustrates the spread of impedance and phase angles measured across all frequencies and settings. Impedance and phase angle errors are shown in Figures (4-5), respectively.

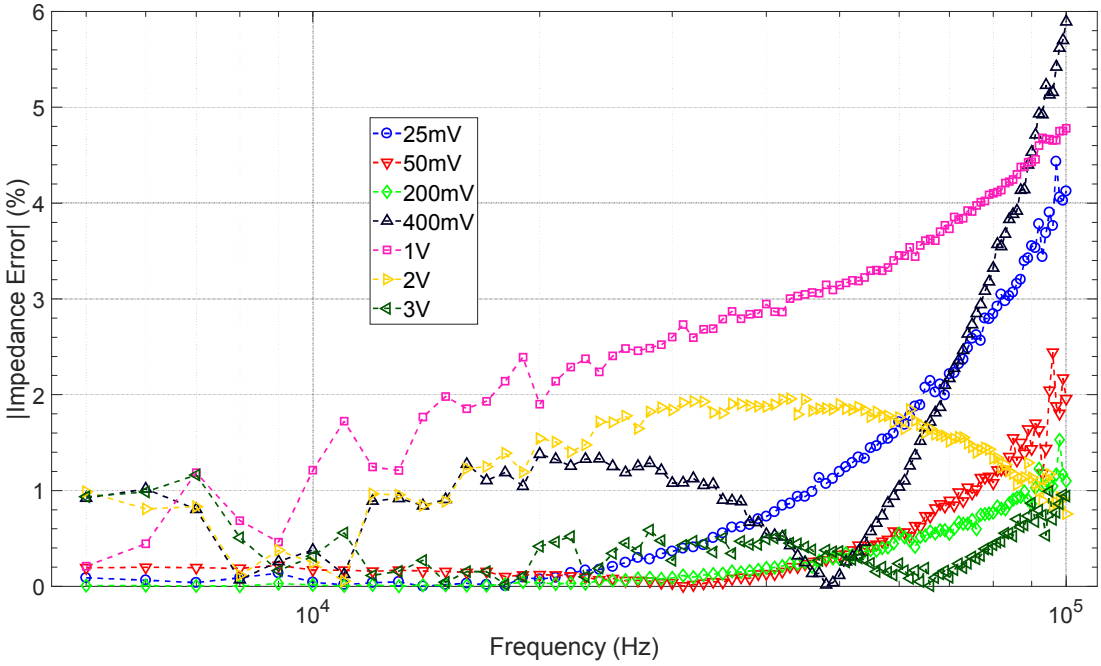

Figure 4. *Absolute impedance error at frequencies between 5 kHz and 100 kHz for all Vpp settings. X-axis is log scale.*

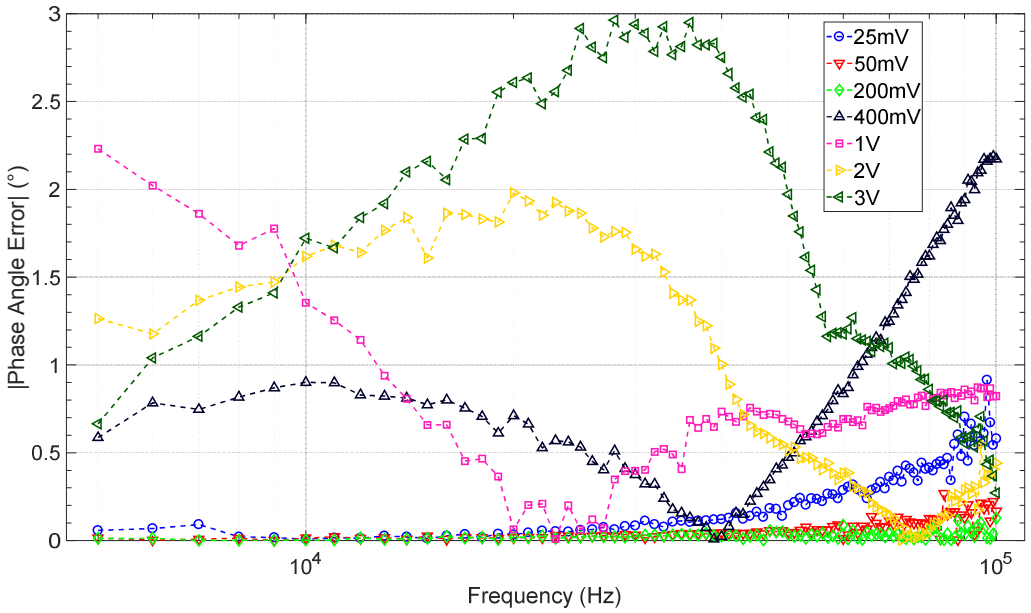

Figure 5. *Absolute phase angle error at frequencies between 5 kHz and 100 kHz for all Vpp settings. X-axis is log scale.*

3.3. Repeatability

Repeated measurements were taken on the volar forearm using two 99% silver coated electrodes with a diameter of 8 mm and a center to center spacing of 14 mm. The purpose of this experiment was to determine the ability of the sensor to obtain consistent repeated measures on living tissues. The skin was initially cleaned with an isopropyl alcohol wipe and allowed to dry for 1 minute. Measurements were taken every two minutes by applying the electrode pair to the same skin area using a 100 gram mass for a total of n=27 repetitions. Between measurements, the electrodes were removed from the skin's surface to avoid the effects of electrode drift [28]. The impedance and phase angle measurements for each frequency and repetition can be seen in Figures (6-7), respectively.

Table 1. *Component values, maximum, and minimum impedance and phase angles measured at each Vpp setting.*

Voltage Setting	R1 (Ω)	R2 (Ω)	C1 (nF)	Min Imp (Ω)	Max Imp (Ω)	Min Phase (°)	Max Phase (°)
25 mV	178	100	0.1000	178	178	-0.0320	-0.6407
50 mV	330	100	0.1000	330	330	-0.0594	-1.1876
200 mV	987	100	0.1000	985	987	-0.1777	-3.5471
400 mV	19795	982	1.0360	1733	16406	-32.2368	-65.4658
1 V	69869	1999	0.3600	4708	54232	-37.8095	-71.0647
2 V	109100	6712	0.2071	9591	87216	-34.4975	-62.9254
3 V	197000	5014	0.1012	16048	165778	-31.7978	-72.0934

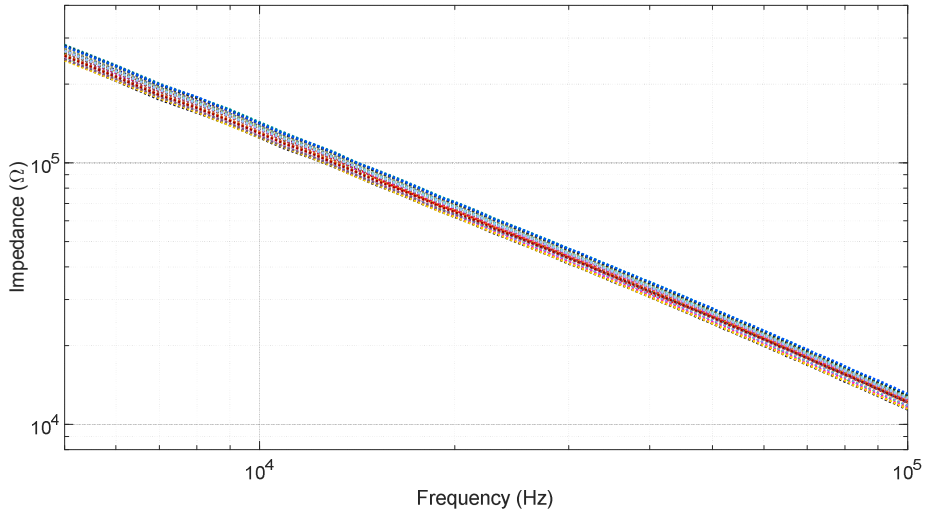

Figure 6*. Impedance measurements on the volar forearm. Both axes are log scale. n = 27.*

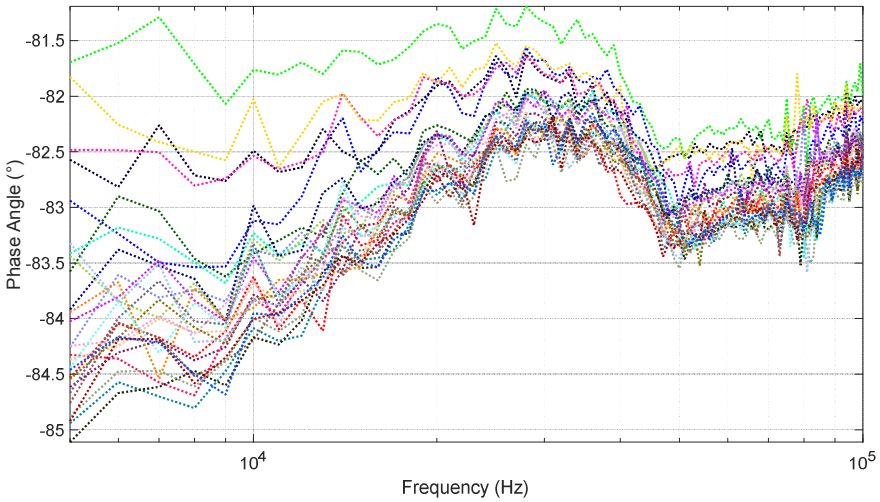

***Figure 7**. Phase angle measurements on the volar forearm. X-axis is log scale. n = 27.*

The maximum relative standard deviation of the measured impedance was found at 6 kHz to be 4.3% while the maximum relative standard deviation of the measured phase angle was found at 5 kHz to be 1.1%. These results indicate good repeatability for human skin measurements. We believe that much of the deviation can be attributed to imperfect repositioning of the electrodes.

3.4. Stability

To determine stability, the device was tested by measuring a single 10 kΩ resistor at each frequency every 10 minutes for 24 hours. Impedance and phase measurements for the 24 hour duration are shown in Figure 8. The standard deviation (σ) and relative standard deviations, for impedance and phase angle at 5 kHz and 100 kHz, are shown in Table 2.

***Table 2.** Standard deviation and relative standard deviation for stability measurements at 5 kHz and 100 kHz.*

Measurement	σ	Relative σ (%)
Impedance 5 kHz	1.8 Ω	0.017
Impedance 100 kHz	2.4 Ω	0.023
Phase Angle 5 kHz	0.005 °	3.973
Phase Angle 100 kHz	0.013 °	0.789

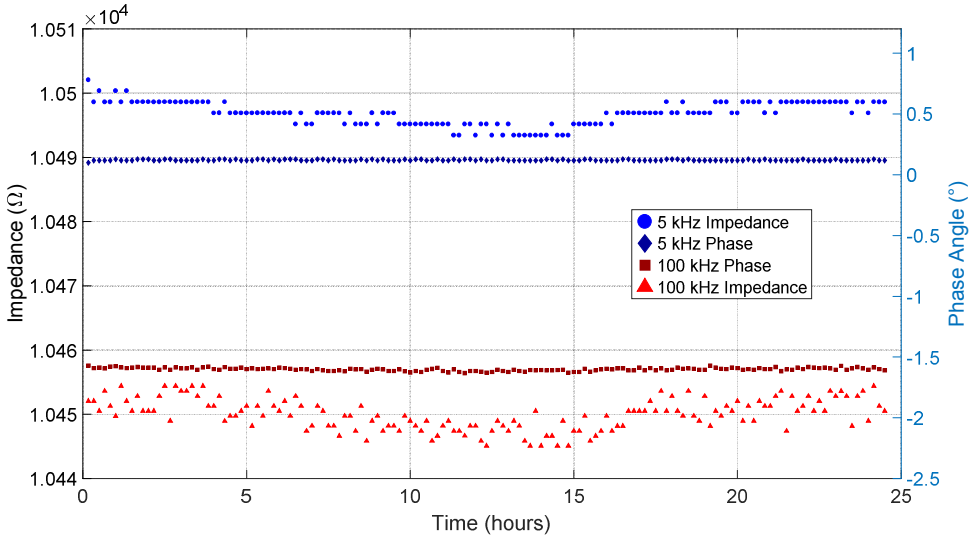

***Figure 8**. Impedance magnitude and phase angle of a 10 kΩ resistor measured at 5 kHz and 100 kHz every 10 minutes for 24 hours.*

3.5. Power Consumption

Power consumption was determined using a 5 V external power supply and an Agilent 34401A Digital Multimeter (DMM). The sensor board, including all components and regulator, idles at 2 mA. With the sensor's regulator disabled, the circuit current can be reduced to less than 1 µA. During sweeps, the sensor consumes a significant 16.4 mA of current, most of which is consumed by the AD5933. For battery operation, sweeps would be performed intermittently to reduce total power consumption. The Arduino Nano and HC-06 Bluetooth chip also consume a significant 23.6 mA current during idle and 37.6 mA when transmitting, but they would not be used in a final consumer-ready version.

4. Discussion

Pressure injuries are painful, increase likelihood of secondary infection, and have a prolonged healing time. These injuries are preventable, however, U.S. healthcare facilities still have an incidence rate of 12% with 40% of all pressure injuries being facility acquired. Current methods for pressure injury detection, such as visual inspection and SEM spot scanning, can lag the pressure loading event by several days. Hence, a continuous device capable of monitoring pressure injury development before irreversible tissue damage has practical significance. Devices designed to monitor interface pressure and temperature have shown promise but individually lack the sensitivity for early detection of pressure injuries [29, 30]. Swisher et al. demonstrated that bioimpedance can be used to monitor pressure injury development, with an optimal measurement frequency of 15 kHz [8]. It is feasible that a device which employs multiple measurement modalities can provide improved sensitivity for pressure injury monitoring. In order to evaluate such a system, a simple, low-cost, and portable sensor for skin bioimpedance measurements has been presented.

The sensor described in this paper is capable of measuring impedances between 180 Ω and 165 kΩ at frequencies between 5 kHz and 100 kHz with impedance and phase accuracies of 6% and 3 °, respectively. We demonstrated that the device is stable by repeated measures for 24 hours with variations as small as 2.4 Ω and 0.013 °. Additionally, we demonstrated that the device can provide consistent skin impedance measurements by measuring the volar forearm with silver electrodes 27 times in one hour. These results are similar to accuracies achieved by other researchers who have used the AD5933 with different AFE's. Margo et al. demonstrated impedance and phase errors of less than 2% and 1.5 °, respectively, when measuring impedances between 100 Ω and 10 kΩ [14]. While these accuracies are superior and are appropriate for their intended application, the reported impedance range is much smaller and the device utilized dual supply op-amps which is unfavorable for portability. Noveletto et al. compared two current source configurations which resulted in impedance and phase errors of less than 3% and 6%, respectively, when measuring impedances between 150 Ω and 1.2 kΩ via a mirrored Howland-modified current source-based AFE [10]. This configuration provides slightly superior circuit performance over a smaller impedance range and is a reasonable alternative for portable bioimpedance if more than 5 V supplies are appropriate for a particular application.

The primary limitation of the sensor's design is the TIA feedback resistor performing two different primary functions. The TIA feedback resistor limits the maximum current that is allowed to pass between the electrodes and amplifies the current passing through an unknown impedance. Hence, the value of the feedback resistor cannot be freely chosen and must always be large enough to ensure user safety. This leads to lower accuracy and a smaller impedance measurement range. A second limitation is the power consumption of the AD5933, which accounts for most of the sensor's current consumption during measurements. Additionally, this sensor cannot be used in a four electrode configuration which limits its flexibility.

While the Arduino Nano and HC-06 were used for their ease of use and low-cost, there are more power efficient processors with built in Bluetooth Low Energy capability, such as the TI CC2650. Future work would optimize system parameters such as measurement frequency, electrode properties, electrode spatial configuration, and measurement intervals in order to optimize the sensitivity of the device to the application of interest.

5. Conclusion

The sensor presented in this paper demonstrates a proof-of-concept for a simple, low-cost, and portable sensor for measuring skin bioimpedance. The sensor demonstrated good accuracy, stability, and repeatability. The simple sensor design can be easily implemented in a portable device with the intention to combine multiple sensing modalities such as local contact pressure, humidity, and temperature for pressure injury monitoring.

Our device has potential for large scale animal and clinical human trials involving pressure ulcer monitoring. Our long term goal is to utilize bioimpedance as one input to a machine learning algorithm to better detect pressure ulcer development and predict an individual's sensitivity to pressure ulcer formation. These algorithms require a significant amount of data for training and our design provides a wireless and cost-effective method for acquiring such a large set of data. Since our device is significantly less expensive, trials could be run at a lower cost with more subjects being monitored simultaneously. In addition to cost benefits, our device is wireless, battery powered, and compact, allowing subjects to remain mobile while still being monitored. Commercial bioimpedance monitors are bulky and typically require a wall power supply. Having a small wireless sensor allows monitoring within and outside of a hospital setting.

Acknowledgements

This research was funded by the National Science Foundation, grant number IGERT DGE 1144804.

References

[1] Van Gilder, C., et al., Results of the 2008-2009 International Pressure Ulcer Prevalence Survey and a 3-year, acute care, unit-specific analysis. Ostomy Wound Manage, 2009. 55(11): p. 39-45.

[2] Brem, H., et al., High cost of stage IV pressure ulcers. Am J Surg, 2010. 200(4): p. 473-7.

[3] Nakagami, G., et al., Predicting delayed pressure ulcer healing using thermography: a prospective cohort study. J Wound Care, 2010. 19(11): p. 465-6, 468, 470 passim.

[4] Aoi, N., et al., Ultrasound assessment of deep tissue injury in pressure ulcers: possible prediction of pressure ulcer progression. Plast Reconstr Surg, 2009. 124(2): p. 540-50.

[5] Baumgarten, M., et al., Validity of pressure ulcer diagnosis using digital photography. Wound Repair Regen, 2009. 17(2): p. 287-90.

[6] Bates-Jensen, B. M., et al., Subepidermal moisture predicts erythema and stage 1 pressure ulcers in nursing home residents: a pilot study. J Am Geriatr Soc, 2007. 55(8): p. 1199-205.

[7] Bates-Jensen, B. M., H. E. McCreath, and V. Pongquan, Subepidermal moisture is associated with early pressure ulcer damage in nursing home residents with dark skin tones: pilot findings. J Wound Ostomy Continence Nurs, 2009. 36(3): p. 277-84.

[8] Swisher, S. L., et al., Impedance sensing device enables early detection of pressure ulcers in vivo. Nat Commun, 2015. 6: p. 6575.

[9] Ching, C. T., et al., Tissue electrical properties monitoring for the prevention of pressure sore. Prosthet Orthot Int, 2011. 35(4): p. 386-94.

[10] Noveletto F., B.-F. P., Dutra D., Analog Front-End for the Integrated Circuit AD5933 Used in Electrical Bioimpedance Measurements, in Latin American Conference on Bioimpedance IFMBE Proceedings. 2016, Springer: Singapore.

[11] Aroom, K. R., et al., Bioimpedance analysis: a guide to simple design and implementation. J Surg Res, 2009. 153(1): p. 23-30.

[12] Bouchaala, D., et al., A high accuracy voltage controlled current source for handheld bioimpedance measurement. 2013. 1-4.

[13] Harder, R., et al., Smart Multi-Frequency Bioelectrical Impedance Spectrometer for BIA and BIVA Applications. IEEE Trans Biomed Circuits Syst, 2016. 10(4): p. 912-9.

[14] Margo, C., et al., A four-electrode low frequency impedance spectroscopy measurement system using the AD5933 measurement chip. Physiol Meas, 2013. 34(4): p. 391-405.

[15] Seoane, F., et al., Simple voltage-controlled current source for wideband electrical bioimpedance spectroscopy: Circuit dependences and limitations. Vol. 22. 2011. 115801.

[16] Armstrong, L. E., et al., Bioimpedance spectroscopy technique: intra-, extracellular, and total body water. Med Sci Sports Exerc, 1997. 29(12): p. 1657-63.

[17] Nescolarde, L., et al., Localized bioimpedance to assess muscle injury. Physiol Meas, 2013. 34(2): p. 237-45.

[18] Khalil, S. F., M. S. Mohktar, and F. Ibrahim, The theory and fundamentals of bioimpedance analysis in clinical status monitoring and diagnosis of diseases. Sensors (Basel), 2014. 14(6): p. 10895-928.

[19] Kyle, U. G., et al., Bioelectrical impedance analysis--part I: review of principles and methods. Clin Nutr, 2004. 23(5): p. 1226-43.

[20] Wagner, D. R., et al., Bioelectrical impedance as a discriminator of pressure ulcer risk. Adv Wound Care, 1996. 9(2): p. 30-7.

[21] Lukaski, H. C. and M. Moore, Bioelectrical impedance assessment of wound healing. J Diabetes Sci Technol, 2012. 6(1): p. 209-12.

[22] Chang, Z. Y., G. M. Pop, and G. M. Meijer, A comparison of two- and four-electrode techniques to characterize blood impedance for the frequency range of 100 Hz to 100 MHz. IEEE Trans Biomed Eng, 2008. 55(3): p. 1247-9.

[23] Schwan, H. P., Electrode polarization impedance and measurements in biological materials. Ann N Y Acad Sci, 1968. 148(1): p. 191-209.

[24] Rosell, J., et al., Skin impedance from 1 Hz to 1 MHz. IEEE Trans Biomed Eng, 1988. 35(8): p. 649-51.

[25] Kim, Y. and H. W. Woo, A prototype system and reconstruction algorithms for electrical impedance technique in medical body imaging. Clin Phys Physiol Meas, 1987. 8 Suppl A: p. 63-70.

[26] Analog Devices. 1 MSPS, 12-Bit Impedance Converter, Network Analyzer. AD5933 datasheet 2017 May 1, 2019]; Available from: https://www.analog.com/media/en/technical-documentation/data-sheets/AD5933.pdf.

[27] Cole, K. S. and R. H. Cole, Dispersion and Absorption in Dielectrics I. Alternating Current Characteristics. The Journal of Chemical Physics, 1941. 9(4): p. 341-351.

[28] Geddes, L. A. and M. E. Valentinuzzi, Temporal changes in electrode impedance while recording the electrocardiogram with "dry" electrodes. Ann Biomed Eng, 1973. 1(3): p. 356-67.

[29] Higashino, T., et al., Combination of thermographic and ultrasonographic assessments for early detection of deep tissue injury. Int Wound J, 2014. 11(5): p. 509-16.

[30] Brienza, D. M., et al., The relationship between pressure ulcer incidence and buttock-seat cushion interface pressure in at-risk elderly wheelchair users. Arch Phys Med Rehabil, 2001. 82(4): p. 529-33.